tor low-pass filter with defected ground structure, Microwave Opt Technol Lett 48 (2006), 405–408.
9. X.Y. Zhang, Q. Xue, and B.J. Hu, Novel bandpass filter with size reduction and harmonic suppression, Microwave Opt Technol Lett 49 (2007), 914–916.
10. F.H. Guan, J.Z. Gu, and X.W. Sun, A bandpass filter with harmonic suppression using SIR and zigzag coupling, Microwave Opt Technol Lett 49 (2007), 2071–2074.
11. J.R. Lee, J.H. Cho, and S.-W Yun, New compact bandpass filter using microstrip λ/4 resonators with open stub inverter, IEEE Microwave Guided Wave Lett 10 (2000), 526–527.
12. J.T. Kuo, and C.Y. Tsai, Periodic stepped-impedance ring resonator (PSIRR) bandpass filter with a miniaturized area and desirable upper stopband characteristics, IEEE Trans Microwave Theory Tech 54 (2006), 117–1112.

INTERNAL MULTIBAND SURFACE-MOUNT MONOPOLE SLOT CHIP ANTENNA FOR MOBILE PHONE APPLICATION

Chih-Hua Chang and Kin-Lu Wong
Department of Electrical Engineering, National Sun Yat-Sen University, Kaohsiung 804, Taiwan, Republic of China; Corresponding author: changch@ema.ee.nsysu.edu.tw

Received 17 October 2007

ABSTRACT: *A multiband monopole slot chip antenna surface-mountable on the system circuit board of the mobile phone is presented. The antenna comprises two monopole slots of different lengths, which are folded and attached onto a foam base in the study. With a compact volume of 30 × 10 × 8 mm³ (2.4 cm³), the antenna can generate a lower band at about 900 MHz to cover GSM operation and a very wide upper band (bandwidth >1 GHz) to cover DCS/PCS/UMTS operation and 2.4 GHz WLAN operation. It is also promising to use a ceramic base of relative permittivity 7.8 to replace the foam base of the antenna. In this case, the antenna volume can be reduced to be 24 × 10 × 8 mm³ (1.92 cm³) only, yet still capable of covering GSM/DCS/PCS/UMTS quad-band operation. The proposed antenna is studied, and obtained results are presented and discussed.* © 2008 Wiley Periodicals, Inc. Microwave Opt Technol Lett 50: 1273–1279, 2008; Published online in Wiley InterScience (www.interscience.wiley.com). DOI 10.1002/mop.23342

Key words: *surface-mount chip antennas; internal mobile phone antennas; monopole; slot antennas; quarter-wavelength slot antennas; multiband antennas*

1. INTRODUCTION

In recent years, promising monopole chip antennas surface-mountable on the system circuit board for mobile phone applications have been reported [1–7]. These monopole chip antennas mainly comprise a dielectric base and metal strips printed on or embedded within the base. The dielectric bases such as the ceramic, plastic, and foam bases have been applied. For this kind of chip antennas, the metal strips are the main resonant or radiating portion, and it is usually not easy to achieve wide operating bandwidths at about 900 and 1800 MHz to cover multiband operation such as GSM (890 ~ 960 MHz), DCS (1710 ~ 1880 MHz), PCS (1850 ~ 1990 MHz), and UMTS (1920 ~ 2170 MHz) for mobile communications [8]. In this article, we demonstrate a novel promising monopole chip antenna using the monopole slot or quarter-wavelength slot as the main resonant element, which is different from the operating principle of the conventional monopole chip antenna [1–7], to generate two wide operating bands at about 900 and 1800 MHz for multiband operation.

The monopole slot antenna is obtained by cutting the printed slot at the edge of the ground plane [9–16]. With comparison to the general slot antenna that is operated as a half-wavelength resonant structure [17–20], the monopole slot antenna has an attractive feature of compact in size for a fixed operating frequency. The promising designs of the monopole slot antenna printed on the system circuit board of the mobile phone for multiband mobile communications have also been devised recently [14, 16]; they can be printed either at the center portion [14] or the top portion [16] of the system circuit board. When printed at the center portion, the monopole slot antenna is easy to provide sufficient bandwidth and efficiency to cover the multiband operation, because in this case maximum coupling to the low-Q chassis dipole type resonance can be obtained [14]. However, this design will also complicate the circuit floor planning and signal line routing on the system circuit board. When printed at the top portion, the reported monopole slot antenna [16] occupies an area of 15 × 40 mm² (6 cm²) on the system circuit board and can cover the desired multiband operation.

In this study, the proposed surface-mount monopole slot chip antenna is to be placed at the top portion of the system circuit board. The antenna comprises two monopole slots of different lengths, which are folded and attached onto a foam base of area 10 × 30 mm² and height 8 mm. The proposed antenna thus occupies a much smaller valuable board space than that of the printed monopole slot antenna in [16] (3 cm² vs. 6 cm²). Moreover, the proposed antenna also provides wide operating bands covering GSM/DCS/PCS/UMTS and 2.4 GHz WLAN (2400 ~ 2484 MHz) operation. Detailed design considerations of the antenna are described in the article, and results for the constructed prototype with a foam base are presented. Effects of various parameters on the antenna performances are analyzed. The promising design of using a ceramic base of relative permittivity 7.8 to replace the foam base of the antenna is also discussed. In this case, the occupied area of the monopole slot chip antenna on the system circuit board can be further reduced.

2. DESIGN CONSIDERATIONS OF PROPOSED ANTENNA

Figure 1(a) shows the geometry of the proposed surface-mount monopole slot chip antenna for the mobile phone. The antenna is to be surface-mounted at the top no-ground region (size 10 × 40 mm²) of the system circuit board, which can reduce the packaging cost of the mobile phone. In the study, a 0.8-mm thick FR4 substrate of size 90 × 40 mm² is used to be considered as the system circuit board. On the front side of the circuit board, there is a printed ground plane of length 80 mm and width 40 mm. These dimensions are reasonable for practical mobile phones. Notice that when the antenna is mounted at the no-ground region, the antenna is grounded to the top edge of the ground plane at point A (the grounding point). The antenna does not occupy the whole no-ground region. It is to be flushed to the left edge of the circuit board, thus leaving an unoccupied area of 10 × 10 mm², which can be used to accommodate the associated electronic components such as the speaker, the lens of the embedded digital camera [21, 22], etc.

The antenna with its metal pattern folded and attached on the surfaces of a foam base (size 30 × 10 × 8 mm³), whose relative permittivity is about that of air, is first studied. From the unfolded metal pattern shown in Figure 1(b), the antenna can be considered to comprise two monopole slots of different lengths. The long monopole slot controls the excitation of the antenna's lower band at about 900 MHz and has a length of 50 mm, with its end portion widened (width $b = 5$ mm and length $a = 12$ mm) to achieve smoother excited equivalent surface magnetic current distributions at the end portion of the monopole slot. This can result in the lowering of the antenna's lower band for a fixed slot length. Effects of the parameters a and b on the antenna's lower band are analyzed in detail in Figure 2 in the next section. Also note that the long monopole slot is bent to be mounted on three adjacent surfaces of the foam base, hence reducing the occupied area of the antenna on the circuit board. For the short monopole slot, it has a length c of 28 mm and a uniform width of 3.5 mm, which controls the excitation of a wide operating band at about 1900 MHz to form as the antenna's upper band. Detailed effects of the length c on controlling the antenna's upper band are given in Figure 4 in the next section. The obtained lower and upper bands of the antenna in this study can cover GSM operation and DCS/PCS/UMTS/WLAN operation, respectively.

The two monopole slots are spaced with a narrow spacing of 1 mm to achieve a compact configuration of the antenna and are series-fed using a 50-Ω microstrip line printed on the back side of the circuit board. The microstrip feedline is located with a distance of 23 mm to the open end of the two monopole slots, and there is a small tuning stub of length 5.5 mm parallel along the outer boundary of the long monopole slot. The location and tuning-stub length of the microstrip feedline are important factors for achieving good impedance matching of the antenna. They can be easily determined from the simulation study [16]; in this study, the simulation software Ansoft HFSS (High Frequency Structure Simulator) [23] is used. The large top matching portion (size 8 × 30 mm^2) is also needed for achieving good impedance matching of the antenna. The suitable size of the top matching portion can also be easily determined from the simulation study [16].

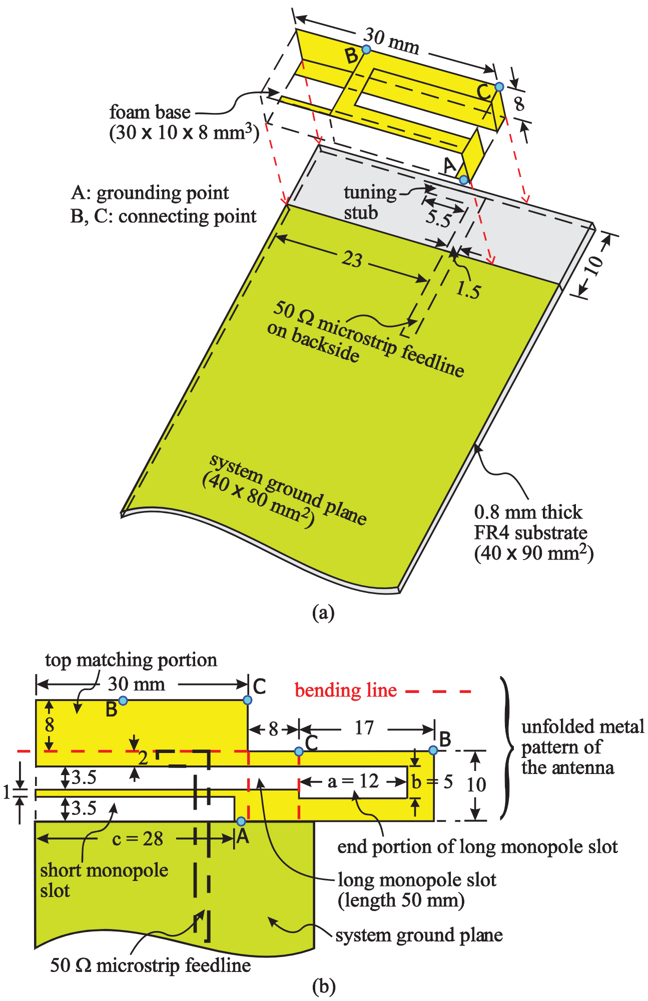

Figure 1 (a) Geometry of the proposed internal multiband surface-mount monopole slot chip antenna for the mobile phone. (b) Dimensions of the metal pattern of the antenna unfolded into a planar structure. [Color figure can be viewed in the online issue, which is available at www.interscience.wiley.com]

3. RESULTS AND DISCUSSION

Figure 3(a) shows the measured and simulated return loss for the constructed prototype with dimensions given in Figure 1. Good agreement between the simulation and measurement is obtained. From the measured data, the antenna's lower band has a 3:1 VSWR (6-dB return loss) bandwidth of 110 MHz (890 ~ 1000 MHz), which covers GSM operation. For the upper band, a very large bandwidth of 1283 (1710 ~ 2993 MHz) is obtained. Moreover, the impedance matching in the 2400 ~ 2500 MHz frequency range is better than 10-dB return loss. This allows the upper band to cover not only DCS/PCS/UMTS operation but also 2.4 GHz WLAN operation. Figure 2(b) shows a comparison of measured

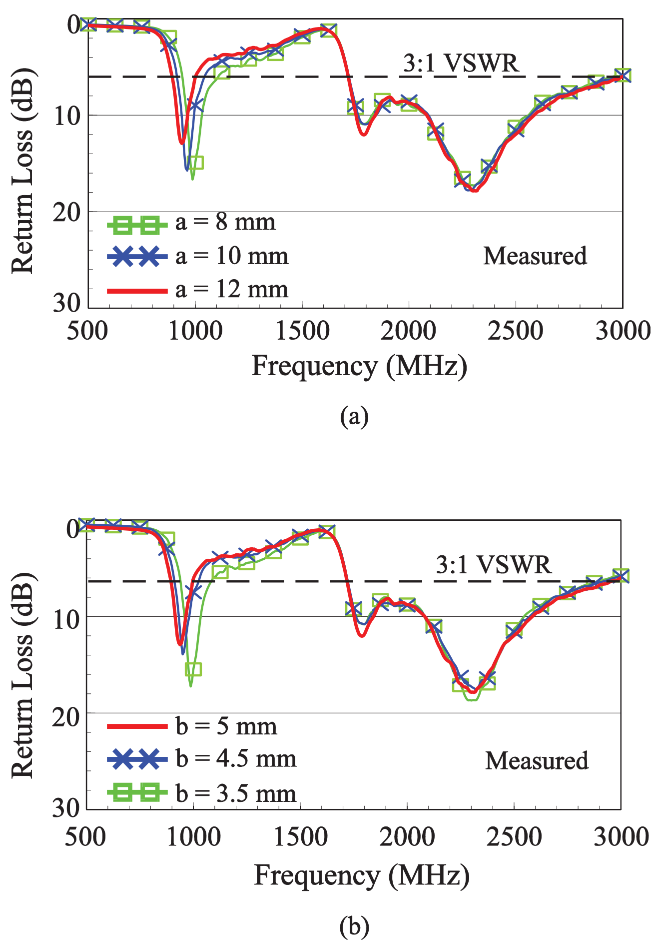

Figure 2 (a) Measured and simulated return loss for the proposed antenna. (b) Comparison of measured return loss for the proposed antenna, the case with the long monopole slot only, and the case with the short monopole slot only; corresponding dimensions are the same as given in Figure 1. [Color figure can be viewed in the online issue, which is available at www.interscience.wiley.com]

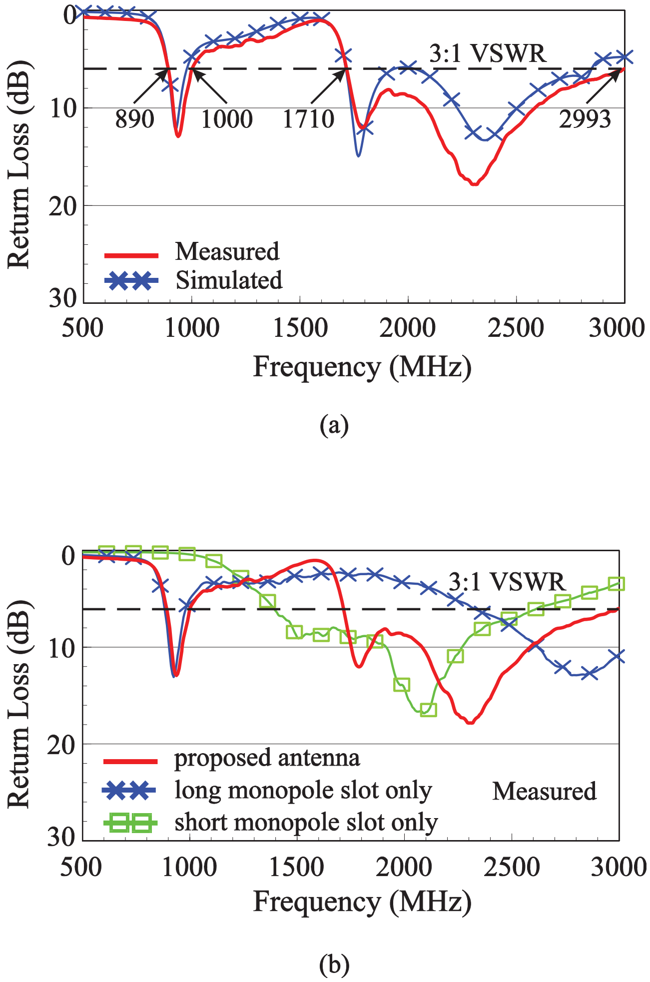

Figure 3 Measured return loss as a function of (a) the length *a*, end-portion length of the long monopole slot and (b) the width *b*, end-portion width of the long monopole slot. [Color figure can be viewed in the online issue, which is available at www.interscience.wiley.com]

return loss for the proposed antenna, the case with the long monopole slot only, and the case with the short monopole slot only; corresponding dimensions of the three cases are the same as given in Figure 1. Results clearly indicate that the antenna's lower

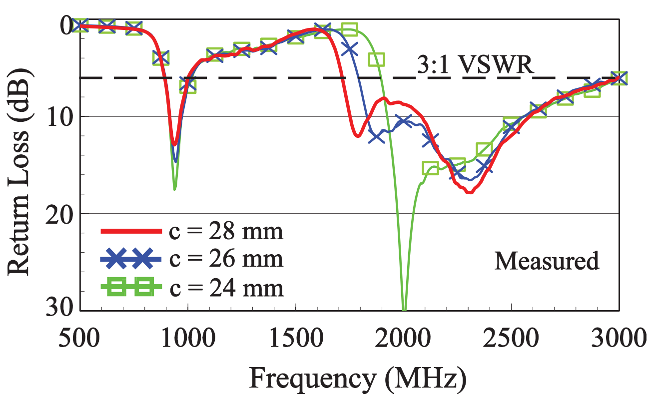

Figure 4 Measured return loss as a function of the length *c* of the short monopole slot; other dimensions are the same as given in Figure 1. [Color figure can be viewed in the online issue, which is available at www.interscience.wiley.com]

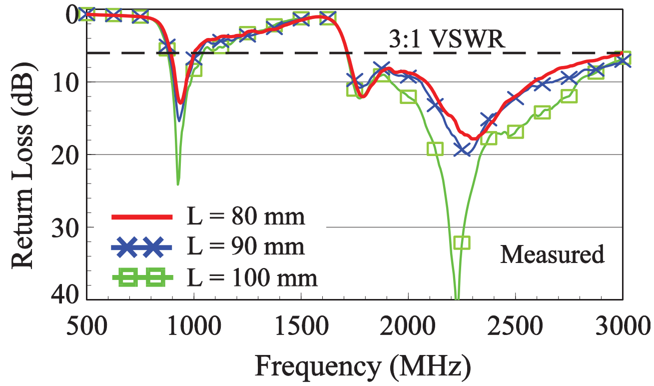

Figure 5 Measured return loss as a function of the groundplane length *L*; other dimensions are the same as given in Figure 1. [Color figure can be viewed in the online issue, which is available at www.interscience.wiley.com]

band is mainly contributed from the long monopole slot. For the case with the short monopole slot only, it generates a very wide bandwidth of larger than 1 GHz, which contributes to the antenna's upper band. The dual-resonance characteristic of the upper band is similar to that observed in [16, 24]; this is mainly owing to the microstrip feedline acting as a virtual short-circuiting across the slot and hence an additional resonance with a shorter resonant slot length is generated in addition to the original resonance associated to the length *c* of the short monopole slot.

Figures 3(a) and 3(b) shows the measured return loss as a function of the length *a* and width *b* of the widened end portion of the long monopole slot. In Figure 3(a), the results for the length *a* varied from

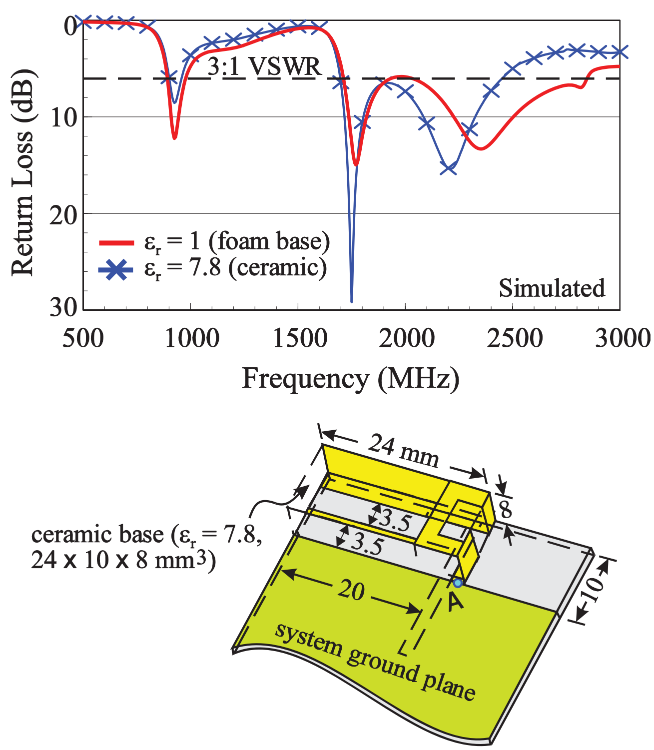

Figure 6 Comparison of simulated return loss for the cases with a foam base (ε_r = 1.0, antenna dimensions given in Fig. 1) and a ceramic chip base (ε_r = 7.8, antenna dimensions given in the figure). [Color figure can be viewed in the online issue, which is available at www.interscience.wiley.com]

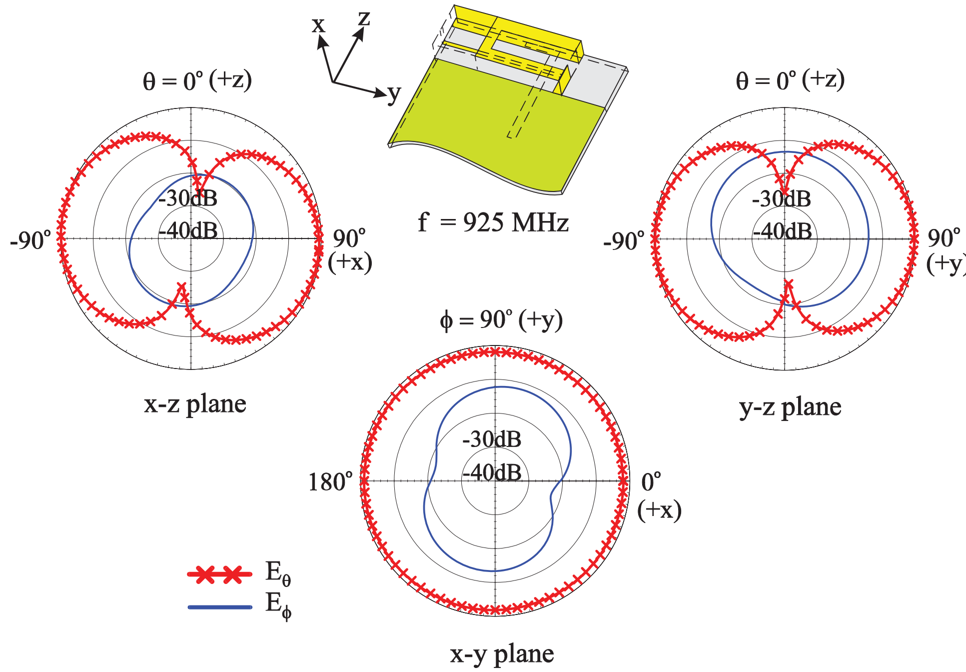

Figure 7 Measured radiation patterns at 925 MHz for the antenna studied in Figure 2. [Color figure can be viewed in the online issue, which is available at www.interscience.wiley.com]

8 to 12 mm are shown. The lower band is shifted to lower frequencies with increasing length *a*. For the upper band, there are almost no effects. Figure 3(b) shows the results for the width *b* varied from 3.5 to 5.0 mm. Again, with an increase in the width *b*, the lower band is shifted to lower frequencies, and the upper band remains almost unchanged. This confirms the expectation that the widened end portion of the long monopole slot can lead to the lowering of the lower band at a fixed slot length discussed in Section 2, while the upper band is generally not affected by the variations in the dimensions of the widened end portion.

Effects of the short monopole slot on the antenna performances are studied in Figure 4, in which the results for the slot length *c* varied from 24 to 28 mm are shown. As expected, the lower band is almost not affected. For the upper band, with an increase in the length *c*, the first resonance of the upper band is shifted to lower frequencies and the second resonance is generally not varied,

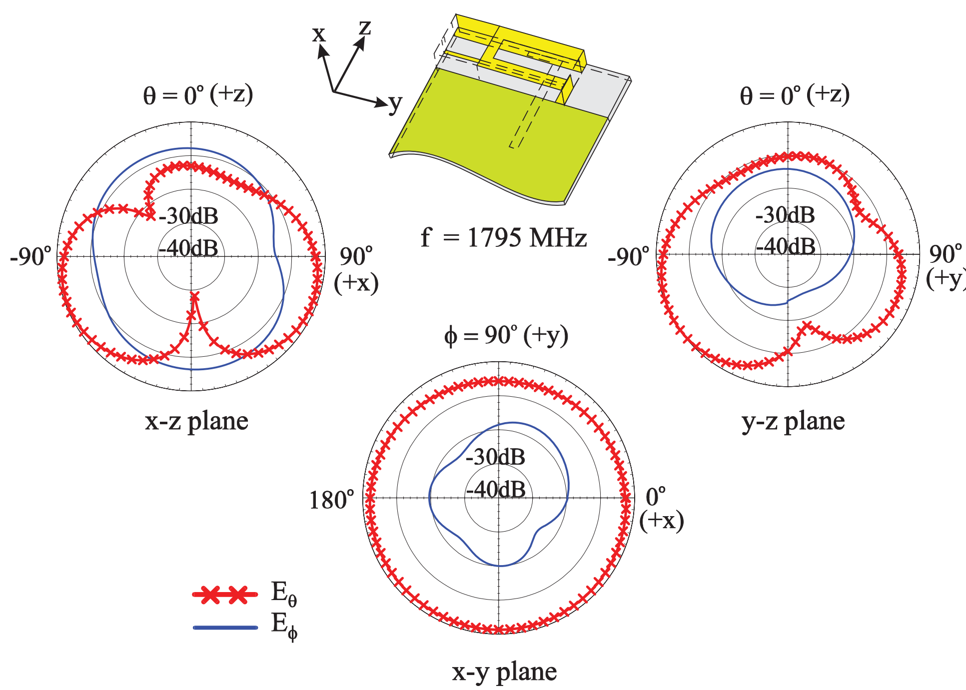

Figure 8 Measured radiation patterns at 1795 MHz for the antenna studied in Figure 2. [Color figure can be viewed in the online issue, which is available at www.interscience.wiley.com]

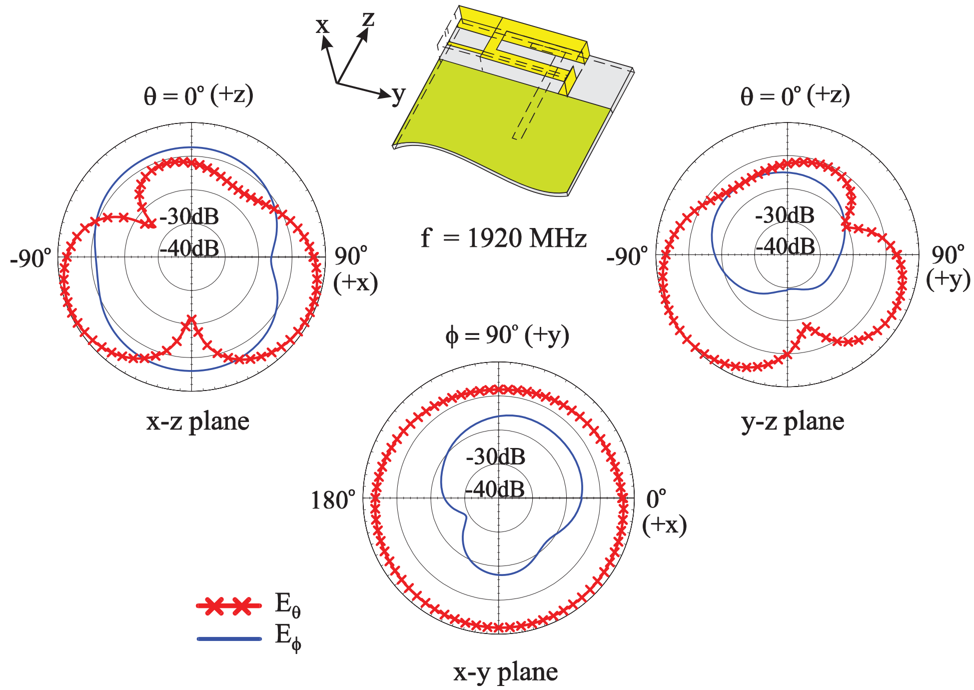

Figure 9 Measured radiation patterns at 1920 MHz for the antenna studied in Figure 2. [Color figure can be viewed in the online issue, which is available at www.interscience.wiley.com]

making the upper band have an enhanced bandwidth. This agrees with the discussion in Section 2, because the first resonance is mainly determined by the slot length *c* and the second resonance is controlled by the slot length from the open end to the microstrip feedline, which is fixed in this study.

Effects of the groundplane length *L* on the measured return loss are studied in Figure 5. Results of the length *L* varied from 80 to 100 mm are shown. There are some variations in the impedance matching of the frequencies over the lower and upper bands. However, the obtained bandwidths are generally about the same. This suggests that the proposed monopole slot chip antenna is suitable for application in the mobile phones with various possible groundplane lengths.

Figure 6 shows the simulated return loss for the cases with a foam base (ε_r = 1.0, antenna dimensions given in Fig. 1) and a ceramic chip base (ε_r = 7.8, antenna dimensions given in the

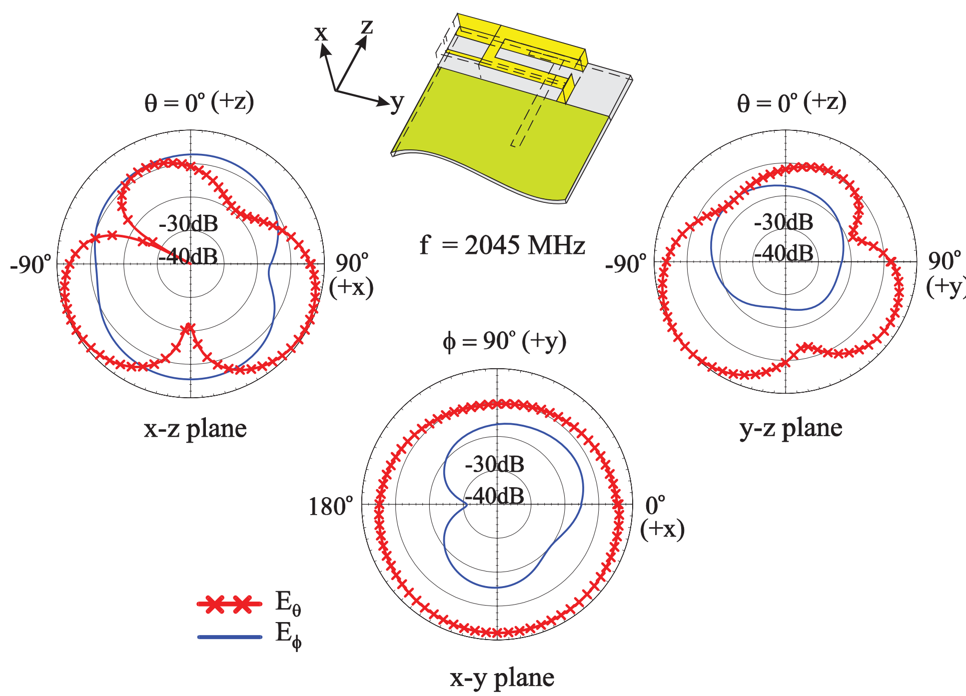

Figure 10 Measured radiation patterns at 2045 MHz for the antenna studied in Figure 2. [Color figure can be viewed in the online issue, which is available at www.interscience.wiley.com]

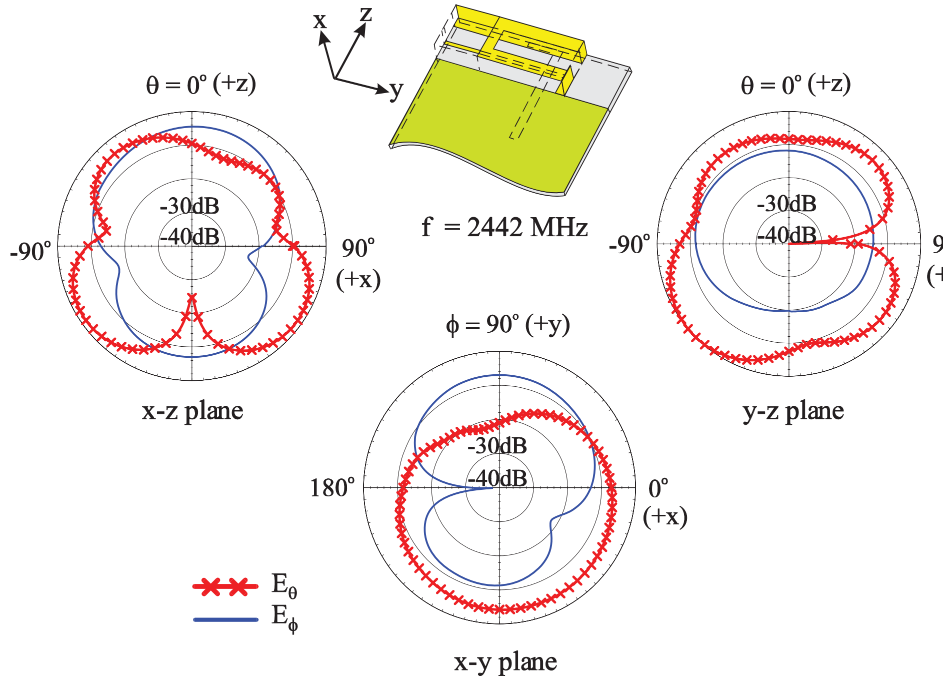

Figure 11 Measured radiation patterns at 2442 MHz for the antenna studied in Figure 2. [Color figure can be viewed in the online issue, which is available at www.interscience.wiley.com]

figure). Notice that the ceramic base occupies an area of 10 × 24 mm^2 only, 30% smaller than that of the foam base. The lengths of the short and long monopole slots are, 34.5 and 22 mm, respectively, for the case with the ceramic base. The sizes of the widened end portion of the long monopole slot and the top matching portion are 2.5 × 5 mm^2 and 8 × 24 mm^2, respectively. The obtained bandwidth of the lower band can still cover GSM operation. For the upper band, the bandwidth is decreased; however, the bandwidth can still cover DCS/PCS/UMTS operation. That is, quad-band operation can be obtained for the proposed monopole slot chip antenna with a ceramic base.

Figures 7–11 plot the measured radiation patterns at 925, 1795, 1920, 2045, and 2442 MHz of the constructed prototype studied in Figure 2. The radiation patterns at other frequencies over the five operating bands studied here are also measured, and similar measured radiation patterns are seen in each operating band of interest. In Figure 7, monopole-like radiation patterns with good omnidirectional radiation in the azimuthal plane (*x*-*y* plane) are seen at 925 MHz, which is similar to those observed for the conventional internal mobile phone antenna [8]. The radiation patterns at 1795 MHz are plotted in Figure 8. More variations in the radiation patterns in the elevation planes (*x*-*z* and *y*-*z* planes) compared to those at 925 MHz are seen; however, small variation in the radiation pattern in the azimuthal plane is still seen, that is, near-omnidirectional radiation is still obtained. Figures 9 and 10 plot the radiation patterns at 1920 and 2045 MHz, respectively. Generally, there are no special distinctions seen among the patterns at 1795, 1920, and 2045 MHz, except that the variations in the radiation patterns in the azimuthal plane are slightly larger at 2045 MHz than those at 1920 and 1795 MHz. These obtained radiation patterns over the upper band are suitable for practical applications in the mobile phones. Figure 11 plots the radiation patterns at 2442 MHz. The amplitudes of the E_θ and E_ϕ components become more

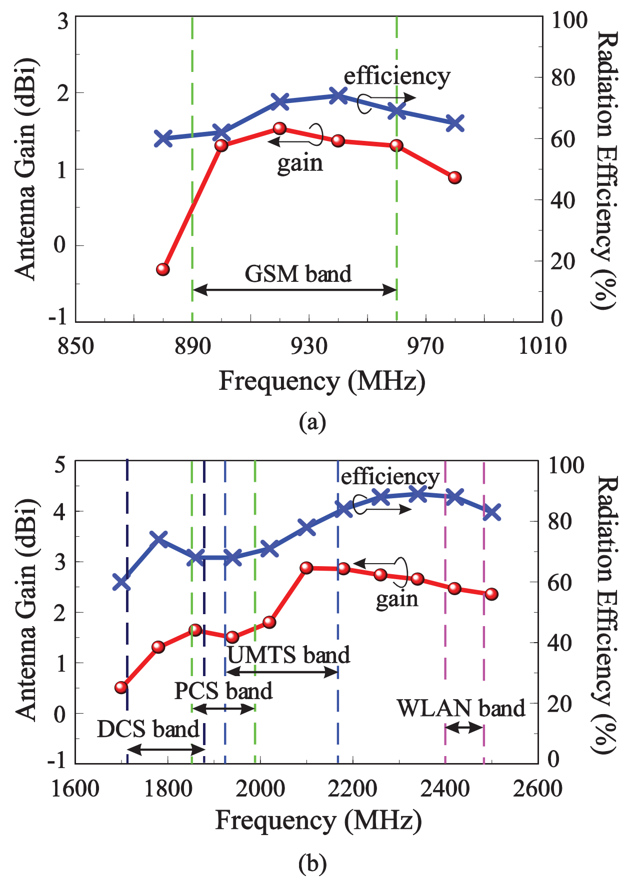

Figure 12 Measured antenna gain and simulated radiation efficiency of the antenna studied in Figure 2. (a) The lower band for GSM operation. (b) The upper band for DCS/PCS/UMTS/WLAN operation. [Color figure can be viewed in the online issue, which is available at www.interscience.wiley.com]

comparable than those shown in Figures 7–10. This is advantageous for WLAN operation, especially in indoor applications where the wave propagation is usually complex.

Figures 12 presents the measured antenna gain and simulated radiation efficiency. Figure 12(a) shows the results over the lower band for GSM operation. The antenna gain is varied from about 0.5–1.5 dBi, and the radiation efficiency is about 60–74%. For the results over the upper band for DCS/PCS/UMTS/WLAN operation, the antenna gain is varied from about 0.6–2.9 dBi, whereas the radiation efficiency is varied in the range of 62–88%.

4. CONCLUSION

A surface-mount multiband monopole slot chip antenna suitable for mobile phone application is presented. Different from the conventional monopole chip antenna using the metal strips as the resonant elements, which is usually not easy to achieve wide operating bandwidths, the proposed monopole slot chip antenna uses two monopole slots as the resonant elements and capable of generating a lower band at 900 MHz for GSM operation and an upper band for DCS/PCS/UMTS/WLAN operation. In addition, the antenna has a simple configuration and is easy to fabricate. It occupies a small area of 30×10 mm^2 on the system circuit board of the mobile phone, which can be further reduced to be 24×10 mm^2 only, when a ceramic base of relative permittivity 7.8 is used to replace the foam base, and the obtained bandwidth can still cover GSM/DCS/PCS/UMTS operation. Good radiation characteristics for frequencies over the antenna's lower and upper bands have also been obtained.

REFERENCES

1. Y.D. Kim and H.M. Lee, Design of compact triple-band meander chip antenna using LTCC technology for mobile handsets, Microwave Opt Technol Lett 48 (2006), 160–162.
2. Y.D. Kim, H.Y. Kim, and H.M. Lee, Dual-band LTCC chip antenna design using stacked meander patch for mobile handsets, Microwave Opt Technol Lett 45 (2005), 271–273.
3. D.S. Yim and S.O. Park, Small internal ceramic chip antenna for IMT-2000 handsets, Electron Lett 39 (2003), 1364–1365.
4. G.Y. Lee, H.T. Chen, and K.L. Wong, A low-cost surface-mount monopole antenna for GSM/DCS operation, Microwave Opt Technol Lett 37 (2003), 2–4.
5. K.L. Wong, S.W. Su, T.W. Chiou, and Y.C. Lin, Dual-band plastic chip antenna for GSM/DCS mobile phones, Microwave Opt Technol Lett 33 (2002), 330–332.
6. S.H. Sim, C.Y. Kang, S.J. Yoon, Y.J. Yoon, and H.J. Kim, Broadband multilayer ceramic chip antenna for handsets, Electron Lett 38 (2002), 205–207.
7. W. Choi, S. Kwon, and B. Lee, Ceramic chip antenna using meander conductor lines, Electron Lett 37 (2001), 933–934.
8. K.L. Wong, Planar antennas for wireless communications, Wiley, New York, 2003.
9. H. Wang, M. Zheng, and S.Q. Zhang, Monopole slot antenna, U.S. Patent No. 6,618,020 B2, (2003).
10. S.K. Sharma, L. Shafai, and N. Jacob, Investigation of wide-band microstrip slot antenna, IEEE Trans Antennas Propag 52 (2004), 865–872.
11. S.L. Latif, L. Shafai, and S.K. Sharma, Bandwidth enhancement and size reduction of microstrip slot antenna, IEEE Trans Antennas Propag 53 (2005), 994–1002.
12. A.P. Zhao and J. Rahola, Quarter-wavelength wideband slot antenna for 3–5 GHz mobile applications, IEEE Antennas Wireless Propag Lett 4 (2005), 421–424.
13. R. Bancroft, Dual slot radiating single feedpoint printed circuit board antenna, U.S. Patent No. 7,129,902 B2, (2006).
14. P. Lindberg, E. Ojefors, and A. Rydberg, Wideband slot antenna for low-profile hand-held terminal applications, Proc 36th European Microwave Conf (EuMC2006), Manchester UK, pp 1698–1701.
15. W.S. Chen and K.Y. Ku, Broadband design of a small non-symmetric ground $\lambda/4$ open slot antenna, Microwave J 50 (2007), 110–120.
16. C.I. Lin, K.L. Wong, and S.H. Yeh, Printed monopole slot antenna for multiband operation in the mobile phone, Proc 2007 IEEE AP-S Int Symp, Honolulu, Hawaii, USA, pp 629–632.
17. P.L. Sun, H.K. Dai, and C.H. Huang, Dual band slot antenna with single feed line, U.S. Patent No. 6,677,909 B2, (2004).
18. C.M. Su, H.T. Chen, and K.L. Wong, Inverted-L slot antenna for WLAN operation, Microwave Opt Technol Lett 37 (2003), 315–316.
19. C.M. Su, H.T. Chen, F.S. Chang, and K.L. Wong, Dual-band slot antenna for 2.4/5.2 GHz WLAN operation, Microwave Opt Technol Lett 35 (2002), 306–308.
20. K.L. Wong, Y.W. Chi, and S.Y. Tu, Internal multiband printed folded slot antenna for mobile phone application, Microwave Opt Technol Lett 49 (2007), 1833–1837.
21. C.M. Su, K.L. Wong, C.L. Tang, and S.H. Yeh, EMC internal patch antenna for UMTS operation in a mobile device, IEEE Trans Antennas Propag 53 (2005), 3836–3839.
22. S.L. Chien, F.R. Hsiao, Y.C. Lin, and K.L. Wong, Planar inverted-F antenna with a hollow shorting cylinder for mobile phone with an embedded camera, Microwave Opt Technol Lett 41 (2004), 418–419.
23. http://www.ansoft.com/products/hf/hfss/, Ansoft Corporation HFSS.
24. N. Behdad and K. Sarabandi, A multiresonant single-element wideband slot antenna, IEEE Antennas Wireless Propag Lett 3 (2004), 5–8.

INTERNAL MULTIBAND LOOP ANTENNA FOR GSM/DCS/PCS/UMTS OPERATION IN THE SMALL-SIZE MOBILE DEVICE

Chun-I Lin and Kin-Lu Wong
Department of Electrical Engineering, National Sun Yat-Sen University, Kaohsiung 804, Taiwan; Corresponding author: linci@ema.ee.nsysu.edu.tw

Received 16 September 2007

ABSTRACT: *An internal multiband loop antenna suitable for application in the small-size mobile device (groundplane length 50 mm only) is presented. Along the loop strip of the antenna, it is configured to have two symmetric meandered sections and a central widened section. With the configured loop strip, three resonant loop modes (0.5-, 1.0-, and 1.5-wavelength loop modes) can be excited to form two wide operating bands centered at about 900 and 1900 MHz for GSM/DCS/PCS/UMTS operation in the small-size mobile device. In addition, the loop antenna along with the short ground plane studied here shows near-omnidirectional radiation patterns in the azimuthal plane for frequencies over the antenna's two wide operating bands, which is different from conventional internal mobile phone antennas and is advantageous for practical applications.* © 2008 Wiley Periodicals, Inc. Microwave Opt Technol Lett 50: 1279–1285, 2008; Published online in Wiley InterScience (www.interscience.wiley.com). DOI 10.1002/mop.23337

Key words: *mobile antennas; loop antennas; internal mobile phone antennas; GSM/DCS/PCS/UMTS operation; multiband operation*

1. INTRODUCTION

Recently, with the rapid growth in mobile communications, multiband operation of the internal antennas for mobile devices such as the mobile phone, smart phone, and the like has become the basic requirement for practical applications. Many related designs of the internal planar inverted-F antenna (PIFA) for multiband operation